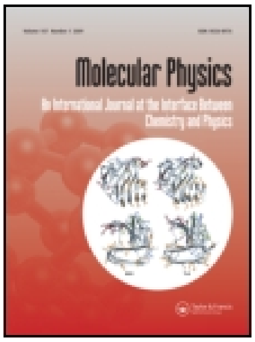

Molecular Physics

ISSN: 0026-8976 (Print) 1362-3028 (Online) Journal homepage: http://www.tandfonline.com/loi/tmph20

New potential energy surfaces for the and states of CH

P. R. Bunker , W. P. Kraemer , S. N. Yurchenko , W. Thiel , C. F. Neese , J. L. Gottfried & Per Jensen

To cite this article: P. R. Bunker , W. P. Kraemer , S. N. Yurchenko , W. Thiel , C. F. Neese , J. L. Gottfried & Per Jensen (2007) New potential energy surfaces for the and states of CH , Molecular Physics, 105:10, 1369-1376, DOI: 10.1080/00268970701344534

To link to this article: https://doi.org/10.1080/00268970701344534

Molecular Physics, Vol. 105, No. 10, 20 May 2007, 1369–1376

Taylor & Francis
Taylor & Francis Group

New potential energy surfaces for the $\tilde{X}$ and $\tilde{A}$ states of CH_2^+

P. R. BUNKER†, W. P. KRAEMER‡, S. N. YURCHENKO§$, W. THIEL§, C. F. NEESE¶,
J. L. GOTTFRIED¶ and PER JENSEN*‖

†Steacie Institute for Molecular Sciences, National Research Council of Canada, Ottawa, Ont.,
Canada K1A 0R6
‡Max-Planck-Institut für Astrophysik, Karl-Schwarzschild-Strasse 1, Postfach 1523,
D–85740 Garching, Germany
§Max-Planck-Institut für Kohlenforschung, Kaiser-Wilhelm-Platz 1, D–45470
Mülheim an der Ruhr, Germany
¶Department of Chemistry, The University of Chicago, Chicago, Illinois 60637, USA
‖Theoretische Chemie, Bergische Universität, D-42097 Wuppertal, Germany

(*Received 28 February 2007; in final form 16 March 2007*)

We report new *ab initio* calculations of the three-dimensional potential energy surfaces for the Renner-effect coupled $\tilde{X}\,^2A_1$ ground electronic state and $\tilde{A}\,^2B_1$ first excited electronic state of the CH_2^+ molecule. We also make an *ab initio* calculation of the spin–orbit coupling surface $A_{SO}(r_{12}, r_{32}, \rho)$ between these states. Using these *ab initio* surfaces in our computer program RENNER, we calculate term values and absorption line intensities, and compare with recently observed high resolution spectra. Adjusting two parameters in the potential surfaces we are able to achieve satisfactory agreement with the experimental results except for those that involve the $\tilde{A}$ state ($v_2^{\rm linear} = 8$, $l = 1$) vibronic level. The implication of this disagreement is discussed.

1. Introduction

This is the tenth in a series of papers by us on the CH_2^+ molecular ion [1–9]. The problem of reconciling the experimentally determined Coulomb explosion image of the molecule with our theoretically predicted image was discussed in [4]; collaboration with experimentalists, using our results as a benchmark [5], allowed all systematic errors in the experiment to be removed and good agreement with our predicted image to be obtained (see [7] and the second, third and fourth paragraphs of the Introduction in [10]). In the course of this previous work we have determined the potential energy surface of the $\tilde{a}\,^4A_2$ excited electronic state of CH_2^+ [8]. Our other papers on CH_2^+ have been concerned with calculating spin–rovibronic term values, and simulating high resolution spectra, for the purpose of assisting and encouraging the experimental spectroscopic characterization of the Renner-coupled $\tilde{X}\,^2A_1$ and $\tilde{A}\,^2B_1$ electronic states of the molecule. We have described the development of our computer program RENNER [3, 11, 12], and have reviewed our work on the Renner effect [7]. A general account, with a bibliography, of the Renner effect is given in Chapter 13 of [13].

Significant experimental spectra of the CH_2^+ molecule have now been obtained by the groups of Oka [14–17] and Merkt [18, 19]. High resolution data is available for the ground and ν_3 (asymmetric stretching) levels of the $\tilde{X}$ ground electronic state, and for the $v_2^{\rm linear}(l) = 8(1)$, 8(3), 9(0) and 9(2) levels of the $\tilde{A}$ excited electronic state.

In this paper we report the results of new *ab initio* calculations of the potential energy surfaces of the $\tilde{X}$ and $\tilde{A}$ states of CH_2^+, and of the spin–orbit coupling surface $A_{SO}(r_{12}, r_{32}, \rho)$ between the states. We use our computer program RENNER to calculate spin–rovibronic term value differences, and compare with the experimental line positions. We make a small optimization of the *ab initio* potential surfaces, by varying two parameters, in a fitting to the data. However, we cannot satisfactorily reproduce the position of the $\tilde{A}$ 8(1) vibronic state and

---

*Corresponding author. Email: jensen@uni-wuppertal.de
$Present address: Institut fur Physikalische Chemie und Elektrochemie, TU Dresden, D-01062 Dresden, Germany.

Molecular Physics
ISSN 0026–8976 print/ISSN 1362–3028 online
http://www.tandf.co.uk/journals
DOI: 10.1080/00268970701344534

it is clearly perturbed by what is almost certainly a high lying $\tilde{X}$ state vibrational level (or levels). To verify this interpretation requires that the $\tilde{X}$ state potential be obtained with greater precision, and this could be achieved if more ground state vibrational energy levels were obtained experimentally.

2. Results

The *ab initio* energies were computed at the CCSD(T) level of coupled cluster theory with inclusion of all single and double substitutions from the Hartree–Fock reference determinant [20] augmented by a perturbative treatment of connected triple excitations [21, 22] using the MOLPRO2002 computer program [23–25]. We used the augmented correlation-consistent polarized valence basis sets, aug-cc-pVTZ and aug-cc-pVQZ developed by Dunning and co-workers [26, 27], in the frozen-core approximation. The energies were extrapolated to the complete basis set limit [28].

For the upper ($\tilde{A}$) state we calculated the potential at 263 geometries, and for the lower ($\tilde{X}$) state we calculated the potential at 429 geometries. For both electronic states, the range of bond lengths covered was from 0.85 to 1.6 Å. The bond angle range was from 110° to 180° for the $\tilde{A}$ state, and from 70° to 180° for the $\tilde{X}$ state. The geometries were chosen so that energies up to 25 000 cm^{-1} above the minimum on the $\tilde{X}$ surface were covered with a uniform grid size. The computer program RENNER uses the analytical expressions for the two potential functions as given in equation (1) of [1], and the optimum values of the parameters in these expressions were determined in one simultaneous least-squares fitting (see [12]) to the *ab initio* energies. The values of the parameters are given in table 1, where $r_{12}^{(\mathrm{ref})}$ is the optimum bond length at linearity; the root-mean-square deviation of the fitting was 15 cm^{-1}. From the fitting we obtain the electronic energy at the minimum of the $\tilde{X}$ state as $-38.707335\,E_\mathrm{h}$. For the $\tilde{X}$ state the equilibrium bond length is calculated as 1.0934 Å, the equilibrium bond angle as 140.44°, and the barrier to linearity (with r relaxed) as 1066.3 cm^{-1}.

In a separate *ab initio* calculation, employing the computer code MOLPRO2002, we determined the spin–orbit coupling factor A_SO between the $\tilde{X}$ and $\tilde{A}$ states, see equation (2) of [11], at 29 geometries with bond lengths from 0.85 to 1.6 Å, and bond angles from 80° to 180°. We used the multi-reference configuration-interaction method [29, 30] with a contracted [5s3p/3s] basis of triple-zeta quality [31], and an active space comprising five electrons in nine molecular orbitals, where the two core orbitals were frozen. Making a least squares fitting to the *ab initio* points, with the analytical expression for $A_\mathrm{SO}(r_{12}, r_{32}, \rho)$ as given in equation (38) of [11], we obtain the following expression (in cm^{-1}):

$$A_\mathrm{SO}(r_{12}, r_{32}, \rho) = 32.24 - 5.06(1 - \cos\rho) - [0.93 + 3.24(1 - \cos\rho)](\Delta r_{12} + \Delta r_{32})\,, \qquad (1)$$

Table 1. The *ab initio* potential energy parameters. The analytical expression for the potential functions is given in equation (1) of [1].

$r_{12}^{(\mathrm{ref})}/\text{Å}$	1.088939(3)[a]	
$a_1/\text{Å}^{-1}$	2.0	
$f_1^{(0)}/\mathrm{cm}^{-1}$	0.0	
$f_{11}^{(0)}/\mathrm{cm}^{-1}$	34591.3(16)	
$f_{13}^{(0)}/\mathrm{cm}^{-1}$	−1401.6(19)	
$f_{111}^{(0)}/\mathrm{cm}^{-1}$	2463.3(12)	
$f_{113}^{(0)}/\mathrm{cm}^{-1}$	−849.3(12)	
$f_{1111}^{(0)}/\mathrm{cm}^{-1}$	4287.4(33)	
$f_{1113}^{(0)}/\mathrm{cm}^{-1}$	−726.3(43)	
$f_{1133}^{(0)}/\mathrm{cm}^{-1}$	−1008.7(59)	
	$\tilde{X}\,{}^2A_1(\sigma = -)$	$\tilde{A}\,{}^2B_1(\sigma = +)$
$f_0^{(1,\sigma)}/\mathrm{cm}^{-1}$	−10030.6(40)	22747.4(61)
$f_0^{(2,\sigma)}/\mathrm{cm}^{-1}$	27525.5(315)	4909.8(412)
$f_0^{(3,\sigma)}/\mathrm{cm}^{-1}$	−21202.3(1009)	2687.9(955)
$f_0^{(4,\sigma)}/\mathrm{cm}^{-1}$	19079.2(1494)	369.8(709)
$f_0^{(5,\sigma)}/\mathrm{cm}^{-1}$	−9007.0(1026)	
$f_0^{(6,\sigma)}/\mathrm{cm}^{-1}$	2175.5(265)	
$f_1^{(1,\sigma)}/\mathrm{cm}^{-1}$	−3013.2(40)	−4484.7(96)
$f_1^{(2,\sigma)}/\mathrm{cm}^{-1}$	2712.1(129)	−1626.8(373)
$f_1^{(3,\sigma)}/\mathrm{cm}^{-1}$	−4380.5(177)	43.2(367)
$f_1^{(4,\sigma)}/\mathrm{cm}^{-1}$	1220.7(78)	
$f_{11}^{(1,\sigma)}/\mathrm{cm}^{-1}$	−585.1(79)	−3670.3(235)
$f_{11}^{(2,\sigma)}/\mathrm{cm}^{-1}$	72.5(170)	−329.8(866)
$f_{11}^{(3,\sigma)}/\mathrm{cm}^{-1}$	−1688.8(108)	−3098.3(1099)
$f_{13}^{(1,\sigma)}/\mathrm{cm}^{-1}$	332.0(94)	2715.5(276)
$f_{13}^{(2,\sigma)}/\mathrm{cm}^{-1}$	1244.5(201)	1410.4(1083)
$f_{13}^{(3,\sigma)}/\mathrm{cm}^{-1}$	1083.8(128)	1706.4(1447)
$f_{111}^{(1,\sigma)}/\mathrm{cm}^{-1}$	−101.1(90)	−4937.9(269)
$f_{111}^{(2,\sigma)}/\mathrm{cm}^{-1}$	−1865.8(102)	−933.0(640)
$f_{113}^{(1,\sigma)}/\mathrm{cm}^{-1}$	−328.2(99)	1569.4(303)
$f_{113}^{(2,\sigma)}/\mathrm{cm}^{-1}$	1593.2(113)	2454.2(791)
$f_{1111}^{(1,\sigma)}/\mathrm{cm}^{-1}$	−2051.5(99)	−5167.4(389)
$f_{1113}^{(1,\sigma)}/\mathrm{cm}^{-1}$	430.1(125)	1735.4(478)
$f_{1133}^{(1,\sigma)}/\mathrm{cm}^{-1}$	1230.3(173)	2352.3(662)

[a] Quantities in parentheses are standard errors in units of the last digit quoted for the parameter.

where $\Delta r_{i2} = r_{i2} - r_{12}^{(\mathrm{ref})}$ and ρ is the supplement of the bond angle. Using this expression for $A_{\mathrm{SO}}(r_{12}, r_{32}, \rho)$, and the analytical fit of our new *ab initio* potential energy surfaces, in the computer program RENNER, we calculated rovibrational energies of the $\tilde{X}$ and $\tilde{A}$ states of the CH_2^+ molecule. The comparison of these results with observed transition wavenumbers (where we restrict attention to transitions between levels for which J is less than 7/2) is given in the column headed $(\mathrm{o}-\mathrm{c})^{\mathrm{b}}$ in tables 2 and 3. In these two tables we use both the linear molecule bending quantum number v_2^{lin} and the bent molecule bending quantum number v_2^{bent} to label the levels. For these two electronic states of CH_2^+, the quantum numbers are related by

$$v_2^{\mathrm{lin}} = 2v_2^{\mathrm{bent}} + |K_a \pm 1|, \tag{2}$$

where the plus sign applies to the upper ($\tilde{A}$) state and the minus sign to the lower ($\tilde{X}$) state. This is a special case (with $\Lambda = 1$) of equation (13–177) of [13], and it follows because the $\tilde{X}$ and $\tilde{A}$ states of CH_2^+ correlate with a Π state at linearity. The angular momentum quantum numbers are related by

$$|l| = K_a, \tag{3}$$

and in linear molecule notation the levels are labelled e or f as $J-(1/2)-K_c$ is odd or even, respectively; *e* levels having parity $+(-1)^{J-1/2}$, and *f* levels having parity $-(-1)^{J-1/2}$. The correlation between the energy level labels of linear and bent triatomic molecules is discussed in section 17.5.2 on p. 633 of [13].

From the observed minus *ab initio* calculated residuals $(\mathrm{o}-\mathrm{c})^{\mathrm{b}}$ in tables 2 and 3, we see that there are four shortcomings in the calculation: the $\tilde{X}(0,0,0)$ state $K_a = 2 \leftarrow 0$ combination differences are too low by about 4 cm^{-1} (previously [2] calculated too low by about 5 cm^{-1}, as pointed out in [19]); the $\tilde{X}$ state ν_3 band wavenumbers are too high by about 1 cm^{-1}; the $\tilde{A}$ state $v_2^{\mathrm{lin}}(l) = 8(3)$, 9(2) and 9(0) vibronic bands are too high by about 30 cm^{-1}; and the 8(1) band is too high by about 70 cm^{-1}. We adjusted two of the *ab initio* parameters in an attempt to rectify the shortcomings. However, the offset of the position of the 8(1) band in relation to the 8(3), 9(0) and 9(2) bands is caused by a perturbation that could not be quantitatively accounted for, and the 8(1) band data was given a weight of zero in these further refinements.

Lowering the barrier to linearity in the $\tilde{X}$ state by about 30 cm^{-1} will largely correct the calculated positions of the $\tilde{A}$ state 8(3), 9(0) and 9(2) levels. As explained on p. 113 of [12], this is most easily achieved

Table 2. Experimentally derived term value differences $\Delta E_{\mathrm{obs}} = E(\tilde{X}, v_1', (v_2^{\mathrm{bent}})', v_3', J', N'_{K_a'K_c'}) - E(\tilde{X}, v_1'', (v_2^{\mathrm{bent}})'', v_3'', J'', N''_{K_a''K_c''})$ for CH_2^+ (in cm^{-1}) and residuals (observed – calculated) from RENNER calculations. Γ_{rve} is the rovibronic symmetry of the level. In this table all term value differences have $v_1' = (v_2^{\mathrm{bent}})' = v_1'' = (v_2^{\mathrm{bent}})'' = v_3'' = 0$.

$(v_2^{\mathrm{lin}})'$	v_3'	J'	$N'_{K_a'K_c'}$	Γ'_{rve}	$(v_2^{\mathrm{lin}})''$	J''	$N''_{K_a''K_c''}$	Γ''_{rve}	$\Delta E^{\mathrm{a}}_{\mathrm{obs}}$	$(\mathrm{o}-\mathrm{c})^{\mathrm{b}}$	$(\mathrm{o}-\mathrm{c})^{\mathrm{c}}$	$(\mathrm{o}-\mathrm{c})^{\mathrm{d}}$
1	0	5/2	2_{21}	B_1	1	3/2	1_{01}	B_1	304.61	4.18	0.29	0.15
1	0	5/2	2_{20}	A_1	1	5/2	2_{02}	A_1	275.11	4.18	0.27	0.13
1	0	5/2	2_{20}	A_1	1	1/2	0_{00}	A_1	319.38	4.18	0.30	0.17
1	0	3/2	2_{20}	A_1	1	3/2	2_{02}	A_1	271.76	3.94	0.13	0.00
1	0	3/2	2_{21}	B_1	1	1/2	1_{01}	B_1	301.28	3.96	0.17	0.04
1	0	5/2	3_{22}	A_1	1	3/2	2_{02}	A_1	317.01	4.05	0.26	0.13
1	0	5/2	3_{21}	B_1	1	5/2	3_{03}	B_1	272.81	4.05	0.22	0.09
1	0	3/2	2_{21}	B_1	1	5/2	3_{03}	B_1	227.52	3.94	0.09	−0.05
1	1	5/2	2_{02}	B_2	1	3/2	1_{01}	B_1	3160.169	−1.008	−2.009	−0.235
1	1	3/2	1_{01}	A_2	1	1/2	0_{00}	A_1	3145.881	−1.020	−2.039	−0.263
1	1	1/2	0_{00}	B_2	1	3/2	1_{01}	B_1	3116.613	−0.996	−2.047	−0.271
0	1	5/2	3_{13}	B_1	0	3/2	2_{12}	B_2	3172.195	−0.893	−2.109	−0.399
0	1	1/2	1_{11}	B_1	0	3/2	2_{12}	B_2	3100.305	−1.068	−2.252	−0.482
0	1	3/2	2_{11}	B_1	0	5/2	3_{12}	B_2	3083.199[e]	−1.719	−2.985	−1.236

[a] The $K_a = 2 \leftarrow 0$ combination differences are from [17], and the ν_3 data are from [14] and [16].

[b] Residuals (in cm^{-1}) obtained from the *ab initio* calculation.

[c] Residuals (in cm^{-1}) from the fitting in which $f_0^{(1,-)}$ is adjusted (to −9888.0 cm^{-1}).

[d] Residuals (in cm^{-1}) from the fitting in which $f_0^{(1,-)}$ and $f_{13}^{(0)}$ are adjusted (to −9883.7 and −1310.7 cm^{-1}, respectively).

[e] Given zero weight in least-squares fitting because this level is perturbed (see [2]).

Table 3. Experimentally derived term value differences $\Delta E_{\mathrm{obs}} = E(\tilde{A}, v_1', (v_2^{\mathrm{lin}})', v_3', J', N'_{K_a'K_c'}) - E(\tilde{X}, v_1'', (v_2^{\mathrm{bent}})'', v_3'', J'', N''_{K_a''K_c''})$ for CH_2^+ (in cm^{-1}) and residuals (observed − calculated) from RENNER calculations. Γ_{rve} is the rovibronic symmetry of the level. In this table all term value differences have $v_1' = v_3' = v_1'' = (v_2^{\mathrm{bent}})'' = v_3'' = 0$.

$(v_2^{\mathrm{bent}})'$	$(v_2^{\mathrm{lin}})'(l')$	J'	$N'_{K_a'K_c'}$	Γ'_{rve}	$(v_2^{\mathrm{lin}})''$	J''	$N''_{K_a''K_c''}$	Γ''_{rve}	ΔE_{obs}[a]	(o − c)[b]	(o − c)[c]	(o − c)[d]
2	$8(3^f)$	5/2	3_{30}	A_2	1	5/2	3_{22}	A_1	10697.5477	−29.7635	−1.3428	−1.3228
2	$8(3^e)$	5/2	3_{31}	B_2	1	3/2	2_{21}	B_1	10742.8314	−29.6276	−1.1827	−1.1641
2	$8(3^f)$	5/2	3_{30}	A_2	1	3/2	2_{20}	A_1	10742.8314	−29.6208	−1.1759	−1.1570
3	$8(1^f)$	3/2	1_{11}	B_2	1	5/2	2_{21}	B_1	10834.4647[e]	−73.2775	−46.4222	
3	$8(1^e)$	3/2	1_{10}	A_2	1	5/2	2_{20}	A_1	10835.4819[e]	−72.5196	−44.8073	
3	$8(1^e)$	3/2	1_{10}	A_2	1	3/2	2_{02}	A_1	11110.5960[e]	−68.3322	−44.5386	
3	$8(1^f)$	3/2	1_{11}	B_2	1	3/2	1_{01}	B_1	11139.0775[e]	−69.0983	−46.1310	
3	$8(1^e)$	3/2	1_{10}	A_2	1	1/2	0_{00}	A_1	11154.8654[e]	−68.3410	−44.5007	
3	$8(1^e)$	1/2	1_{11}	B_2	1	3/2	2_{21}	B_1	10838.8883[e]	−73.1962	−45.3045	
3	$8(1^f)$	1/2	1_{10}	A_2	1	3/2	2_{20}	A_1	10839.8482[e]	−72.5421	−43.9174	
3	$8(1^f)$	1/2	1_{10}	A_2	1	3/2	2_{02}	A_1	11111.6050[e]	−68.6030	−43.7907	
3	$8(1^e)$	1/2	1_{11}	B_2	1	3/2	1_{01}	B_1	11140.1702[e]	−69.2388	−45.1288	
3	$8(1^e)$	5/2	2_{11}	B_2	1	5/2	2_{21}	B_1	10864.0665[e]	−72.7054	−44.4874	
3	$8(1^f)$	5/2	2_{12}	A_2	1	5/2	2_{02}	A_1	11136.0852[e]	−70.7454	−49.1742	
3	$8(1^e)$	5/2	2_{11}	B_2	1	3/2	1_{01}	B_1	11168.6830[e]	−68.5225	−44.1926	
3	$8(1^e)$	3/2	2_{12}	A_2	1	5/2	3_{22}	A_1	10819.6877[e]	−74.8336	−48.7221	
3	$8(1^f)$	3/2	2_{11}	B_2	1	5/2	3_{21}	B_1	10822.6385[e]	−72.7816	−44.1630	
3	$8(1^f)$	3/2	2_{11}	B_2	1	3/2	2_{21}	B_1	10867.9238[e]	−72.6786	−44.0336	
3	$8(1^f)$	3/2	2_{11}	B_2	1	5/2	3_{03}	B_1	11095.4486[e]	−68.7291	−43.9422	
3	$8(1^e)$	3/2	2_{12}	A_2	1	3/2	2_{02}	A_1	11136.7001[e]	−70.7799	−48.4566	
3	$8(1^f)$	3/2	2_{11}	B_2	1	1/2	1_{01}	B_1	11169.1970[e]	−68.7304	−43.8671	
3	$8(1^e)$	5/2	3_{13}	B_2	1	5/2	3_{21}	B_1	10859.0846[e]	−77.2066	−53.9099	
3	$8(1^f)$	5/2	3_{12}	A_2	1	5/2	3_{22}	A_1	10866.2110[e]	−72.0310	−43.1393	
3	$8(1^e)$	5/2	3_{13}	B_2	1	5/2	3_{03}	B_1	11131.8905[e]	−73.1583	−53.6934	
3	$8(1^f)$	5/2	3_{12}	A_2	1	3/2	2_{02}	A_1	11183.2266[e]	−67.9741	−42.8706	
3	$9(2^e)$	5/2	2_{21}	A_1	0	5/2	2_{11}	A_2	12145.7577	−25.4644	−3.8328	−3.9521
3	$9(2^f)$	5/2	2_{20}	B_1	0	5/2	2_{12}	B_2	12148.1639	−25.5687	−3.8687	−4.0278
3	$9(2^f)$	5/2	2_{20}	B_1	0	3/2	1_{10}	B_2	12175.7841	−25.5354	−3.8194	−3.9790
3	$9(2^e)$	5/2	2_{21}	A_1	0	3/2	1_{11}	A_2	12176.6273	−25.5255	−3.8136	−3.9316
3	$9(2^f)$	3/2	2_{21}	A_1	0	3/2	2_{11}	A_2	12152.1844	−25.3450	−2.2750	−2.4389
3	$9(2^e)$	3/2	2_{20}	B_1	0	3/2	2_{12}	B_2	12154.1943	−25.8342	−2.7008	−2.8635
3	$9(2^e)$	3/2	2_{20}	B_1	0	1/2	1_{10}	B_2	12183.0590	−25.6645	−2.5753	−2.7406
3	$9(2^f)$	3/2	2_{21}	A_1	0	1/2	1_{11}	A_2	12183.9023	−25.6645	−2.5749	−2.7395
3	$9(2^f)$	5/2	3_{22}	B_1	0	5/2	3_{12}	B_2	12146.8561	−26.3490	−3.2313	−3.3932
3	$9(2^e)$	5/2	3_{21}	A_1	0	5/2	3_{13}	A_2	12151.5452	−26.6371	−3.3500	−3.5104
3	$9(2^e)$	5/2	3_{21}	A_1	0	3/2	2_{11}	A_2	12192.4202	−26.4911	−3.2333	−3.3962
3	$9(2^f)$	5/2	3_{22}	B_1	0	3/2	2_{12}	B_2	12195.0335	−26.4140	−3.1824	−3.3427
4	$9(0^f)$	1/2	0_{00}	B_1	0	3/2	1_{10}	B_2	12241.8269	−29.3207	3.8088	3.9057
4	$9(0^f)$	3/2	1_{01}	A_1	0	5/2	2_{11}	A_2	12225.4328	−29.7947	3.2125	3.3068
4	$9(0^f)$	3/2	1_{01}	A_1	0	3/2	1_{11}	A_2	12256.3106	−29.8476	3.2399	3.3355
4	$9(0^e)$	1/2	1_{01}	A_1	0	3/2	2_{11}	A_2	12227.1347	−29.2836	3.6605	3.7529
4	$9(0^e)$	1/2	1_{01}	A_1	0	1/2	1_{11}	A_2	12258.8577	−29.5981	3.3657	3.4573
4	$9(0^f)$	5/2	2_{02}	B_1	0	5/2	2_{12}	B_2	12255.2564	−30.8488	2.0820	2.1741
4	$9(0^f)$	5/2	2_{02}	B_1	0	3/2	1_{10}	B_2	12282.8655	−30.8267	2.1203	2.2118
4	$9(0^e)$	3/2	2_{02}	B_1	0	5/2	3_{12}	B_2	12208.3769	−30.6594	2.0900	2.1776
4	$9(0^e)$	3/2	2_{02}	B_1	0	3/2	2_{12}	B_2	12256.5514	−30.7274	2.1360	2.2252
4	$9(0^e)$	3/2	2_{02}	B_1	0	1/2	1_{10}	B_2	12285.4015	−30.5723	2.2468	2.3335
4	$9(0^e)$	5/2	3_{03}	A_1	0	5/2	3_{13}	A_2	12254.3826	−32.2500	0.3937	0.4790
4	$9(0^e)$	5/2	3_{03}	A_1	0	3/2	2_{11}	A_2	12295.2414	−32.1202	0.4942	0.5770

[a] From [17].

[b] Residuals (in cm^{-1}) obtained from the *ab initio* calculation.

[c] Residuals (in cm^{-1}) from the fitting in which $f_0^{(1,-)}$ is adjusted (to $-9888.0\,\mathrm{cm}^{-1}$).

[d] Residuals (in cm^{-1}) from the fitting in which $f_0^{(1,-)}$ and $f_{13}^{(0)}$ are adjusted (to -9883.7 and $-1310.7\,\mathrm{cm}^{-1}$, respectively). No entries given for the 8(1) vibronic state because of heavy mixing, see text.

[e] Given zero weight in the least-squares fittings because this level is perturbed (see [2]).

by increasing the ground state bending parameter $f_0^{(1,-)}$, and thus we first adjusted $f_0^{(1,-)}$ in a least-squares fitting to the data in tables 2 and 3. The value obtained for $f_0^{(1,-)}$ was $-9888.0(1.9)\,\mathrm{cm}^{-1}$, where the number in parentheses is the standard error. This adjustment reduces the ground state barrier to linearity by 32 to $1034\,\mathrm{cm}^{-1}$, and the equilibrium bond angle is increased by 0.4° to 140.8°. The observed-minus-calculated residuals obtained are given in the column headed $(\mathrm{o}-\mathrm{c})^{\mathrm{c}}$ in tables 2 and 3, and we see that as well as improving the agreement for the positions of the 8(3), 9(0) and 9(2) bands, this adjustment to the ground state bending potential has greatly improved the calculation of the ground state $K_a = 2 \leftarrow 0$ combination differences. It has, however, moved the ν_3 band further from its observed position. Thus, in a second least-squares refinement, we adjusted both $f_0^{(1,-)}$ and $f_{13}^{(0)}$. The values obtained for the parameters were $f_0^{(1,-)} = -9883.7(2.8)\,\mathrm{cm}^{-1}$ and $f_{13}^{(0)} = -1310.7(44.0)\,\mathrm{cm}^{-1}$. The observed-minus-calculated residuals are given in the column headed $(\mathrm{o}-\mathrm{c})^{\mathrm{d}}$ in tables 2 and 3, and we see that the calculated ground state $K_a = 2 \leftarrow 0$ combination differences, and the calculated ν_3 band transitions, are significantly closer to experiment. For the final adjusted potentials, the barrier to linearity is $1033.0\,\mathrm{cm}^{-1}$, the equilibrium bond length is 1.0933 Å, and the equilibrium bond angle is 140.81° in the ground state.

Figure 1 shows the bending cross-sections through the final adjusted potential energy surfaces with the bond lengths held fixed at their optimum value at linearity of 1.0889 Å. We have also drawn in the calculated positions of all the $\tilde{X}$ state $(0, v_2^{\mathrm{bent}}, 0)$ 0_{00} $(J = 1/2)$ bending levels up to that with $v_2^{\mathrm{bent}} = 12$, and the calculated positions of the lowest rovibronic level in each of the $\tilde{A}$ state vibronic levels having $v_2^{\mathrm{linear}}(l) = 8(3)$, 8(1), 9(2), 9(0) and 10(3). In order to refer these term values to the minimum of the bending potential, rather than to the lowest level, we have added the bending zero-point energy which we calculate to be $543.96\,\mathrm{cm}^{-1}$. One might infer from the positions of the levels in this figure that, since the lowest rovibronic level of the $\tilde{A}$ 8(1) vibronic state is not far above that of the 0_{00} $(J = 1/2)$ level of the $\tilde{X}$ (0, 8, 0) vibronic state, a significant perturbation between these states could occur. However, it is the $\tilde{X}$ (0, 8, 0) $K_a = 1$ state, not the $\tilde{X}$ (0, 8, 0) $K_a = 0$ state, that has the correct symmetry to perturb the $\tilde{A}$ 8(1) vibronic state, and in our calculation the $\tilde{X}$ (0, 8, 0) $K_a = 1$ state is nearly $760\,\mathrm{cm}^{-1}$ below the $\tilde{X}$ (0, 8, 0) $K_a = 0$ state (see figure 13-10 in [13]).

To show the density of the $\tilde{X}$ state vibrational levels as a function of their energy, we give the calculated positions of all the 0_{00} $(J = 1/2)$ rovibronic energies for the $\tilde{X}$ state, up to that having $(v_1, v_2^{\mathrm{bent}}, v_3) = (0, 9, 0)$, using the final adjusted potential energy surfaces, in table 4.

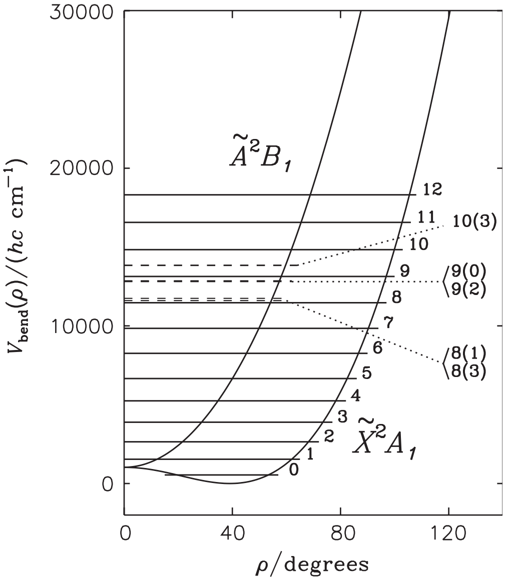

Figure 1. Bending cross-sections through the final adjusted potential energy surfaces (with $f_0^{(1,-)} = -9883.7\,\mathrm{cm}^{-1}$ and $f_{13}^{(0)} = -1310.7\,\mathrm{cm}^{-1}$) with the bond lengths held fixed at 1.0889 Å (the optimum value at linearity). The calculated $\tilde{X}$ $(0, v_2, 0)$ 0_{00} $(J = 1/2)$ levels having $v_2^{\mathrm{bent}} = 0$ through 12 are drawn in, as are the lowest rovibronic levels of some of the calculated $\tilde{A}$ state levels $v_2^{\mathrm{linear}}(l)$ having $v_2^{\mathrm{linear}} = 8$, 9 and 10. The bending zero point energy of $543.96\,\mathrm{cm}^{-1}$ has been added to all energies so that they are referred to the minimum of the $\tilde{X}$ state bending potential.

3. Discussion

Using the *ab initio* dipole moment and transition moment surfaces, as calculated in [3], with the final adjusted potential surfaces that we have obtained here, we can calculate the positions and absorption intensities of all spectral lines arising from transitions within and between the $\tilde{X}$ and $\tilde{A}$ states of CH_2^+ at any temperature (assuming Boltzmann equilibrium). In table 5 we list the results of a calculation, with $N(\mathrm{max}) = 10$, of the positions and absorption intensities of all lines having intensity greater than $0.75\,\mathrm{km\,mol}^{-1}$ in the region from 10 500 to $12\,500\,\mathrm{cm}^{-1}$ at 400 K. Using these final potentials the $(v_1, v_2^{\mathrm{bent}}, v_3) = (3, 3, 0)$, $K_a = 1$ level of the $\tilde{X}$ state is strongly mixed with the $v_2^{\mathrm{linear}}(l) = 8(1)$ level of the $\tilde{A}$ state; this latter level has $v_2^{\mathrm{bent}} = 3$. The mixing is so strong that the eigenfunctions of both levels have the $\tilde{A}$ 8(1) basis state as that with the largest coefficient; in this circumstance, the computer program RENNER labels both levels as being the $\tilde{A}$ 8(1) vibronic state. This is the reason why there are two doublets in table 5, between 11 172 and $11\,215\,\mathrm{cm}^{-1}$, for which the two

Table 4. The term values E (in cm^{-1}) for $\tilde{X}$-state $J = 1/2\ 0_{00}$ rovibronic levels calculated using the adjusted potential surfaces with $f_0^{(1,-)} = -9883.7\,\mathrm{cm}^{-1}$ and $f_{13}^{(0)} = -1310.7\,\mathrm{cm}^{-1}$. Γ_{rve} is the rovibronic symmetry of the level and v_2 is v_2^{bent}.

Γ_{rve}	(v_1, v_2, v_3)	E	Γ_{rve}	(v_1, v_2, v_3)	E
A_1	(0, 0, 0)	0.0[a]	A_1	(0, 7, 0)	9297.6
A_1	(0, 1, 0)	997.0	A_1	(0, 3, 2)	9391.0
A_1	(0, 2, 0)	2102.2	A_1	(3, 1, 0)	9476.8
A_1	(1, 0, 0)	2899.5	B_2	(2, 1, 1)	9603.3
B_2	(0, 0, 1)	3131.6	A_1	(1, 1, 2)	9856.7
A_1	(0, 3, 0)	3346.4	B_2	(0, 1, 3)	10157.9
A_1	(1, 1, 0)	3888.6	A_1	(2, 4, 0)	10247.1
B_2	(0, 1, 1)	4111.9	B_2	(1, 4, 1)	10405.4
A_1	(0, 4, 0)	4701.0	A_1	(1, 6, 0)	10492.5
A_1	(1, 2, 0)	4986.8	A_1	(3, 2, 0)	10573.6
B_2	(0, 2, 1)	5187.7	B_2	(0, 6, 1)	10632.8
A_1	(2, 0, 0)	5736.4	A_1	(0, 4, 2)	10672.9
B_2	(1, 0, 1)	5923.4	B_2	(2, 2, 1)	10679.0
A_1	(0, 5, 0)	6114.7	A_1	(1, 2, 2)	10898.6
A_1	(0, 0, 2)	6202.4	A_1	(0, 8, 0)	10923.9
A_1	(1, 3, 0)	6251.6	B_2	(0, 2, 3)	11178.2
B_2	(0, 3, 1)	6397.2	A_1	(4, 0, 0)	11194.7
A_1	(2, 1, 0)	6717.1	B_2	(3, 0, 1)	11275.7
B_2	(1, 1, 1)	6894.9	A_1	(2, 0, 2)	11531.0
A_1	(0, 1, 2)	7166.9	B_2	(2, 3, 1)	11730.0
A_1	(1, 4, 0)	7501.2	A_1	(2, 5, 0)[b]	11598.5
A_1	(0, 6, 0)	7714.4	A_1	(3, 3, 0)[b]	11796.2
B_2	(0, 4, 1)	7714.5	B_2	(1, 0, 3)	11814.6
A_1	(2, 2, 0)	7811.6	B_2	(1, 5, 1)	11897.3
B_2	(1, 2, 1)	7962.8	A_1	(1, 3, 2)	11988.5
A_1	(0, 2, 2)	8214.7	A_1	(1, 7, 0)	12064.6
A_1	(3, 0, 0)	8505.4	A_1	(0, 5, 2)	12128.6
B_2	(2, 0, 1)	8641.1	A_1	(0, 0, 4)	12147.6
A_1	(1, 5, 0)	8887.1	A_1	(4, 1, 0)	12155.8
A_1	(1, 0, 2)	8900.5	B_2	(0, 7, 1)	12191.9
A_1	(2, 3, 0)	9062.6	B_2	(3, 1, 1)	12228.1
B_2	(1, 3, 1)	9077.2	B_2	(0, 3, 3)	12321.0
B_2	(0, 5, 1)	9203.9	A_1	(2, 1, 2)	12480.4
B_2	(0, 0, 3)	9208.6	A_1	(0, 9, 0)	12591.1

[a] Full three-dimensional zero-point energy = 3637.4 cm^{-1} relative to the Born–Oppenheimer minimum.

[b] These levels are in strong Fermi resonance and both gain the label (3, 3, 0) in the output of RENNER.

members have the same assignment. All lines arising from transitions to the $\tilde{A}$ 8(1) level would be doublets if we lowered the intensity threshold. Making a similar calculation of line positions and absorption intensities using either our unadjusted *ab initio* potential energy surfaces, or those with $f_0^{(1,-)}$ adjusted to $-9888.0\,\mathrm{cm}^{-1}$, does not lead to the presence of doublets for which the two members have the same assignment, because there is no strong mixing of the $\tilde{X}(3,3,0)$ $K_a = 1$ and $\tilde{A}$ 8(1) levels for those potentials even though they are both only very slightly different from our final potentials. As an aside, if we lower the intensity threshold, we find that the next most intense band in this region is that involving the $\tilde{A}$ 9(4) state, for which we calculate 25 lines between 11 380 and 11 500 cm^{-1} with intensities from 0.1 to 0.6 km mol^{-1}; transitions to this vibronic state have not yet been identified in the observed spectrum.

We have been unable to achieve satisfactory agreement for the position of the $\tilde{A}$ 8(1) vibronic state by adjusting the parameters that define our new *ab initio* potential surfaces, in a fitting to the experimental term value differences. It is clear that this state is perturbed and pushed down by a high lying level, or levels, of the $\tilde{X}$ state, but in tests we have found that the $\tilde{X}(3,3,0)$ K_a=1 state alone cannot exert enough of a perturbation. It could be that the $\tilde{X}(2,5,0)$ state also participates in this perturbation via a Fermi resonance with the $\tilde{X}(3,3,0)$ state, or that the bulk of the perturbation is caused by another $\tilde{X}$ state vibrational level.

Table 5. Calculated lower term values E'' (in cm^{-1}), transition wavenumbers ν (in cm^{-1}), line strengths S (in D^2), and intensities I (in $\mathrm{km\,mol}^{-1}$) for selected CH_2^+ transitions with $v_1' = v_3' = v_1'' = v_3'' = 0$.

$(v_2^{\mathrm{bent}})'$	$(v_2^{\mathrm{lin}})'(l')$	J'	$N'_{K_a'K_c'}$	Γ'_{rve}	$(v_2^{\mathrm{lin}})''$	J''	$N''_{K_a''K_c''}$	Γ''_{rve}	E''	ν	S	I
2	$8(3^{\mathrm{f}})$	7/2	3_{31}	B_2	1	5/2	2_{21}	B_1	319.208	10738.297	0.03142	1.557
2	$8(3^{\mathrm{e}})$	5/2	3_{31}	B_2	1	3/2	2_{21}	B_1	315.989	10743.988	0.02265	1.136
2	$8(3^{\mathrm{e}})$	9/2	4_{31}	B_2	1	7/2	3_{21}	B_1	363.340	10750.618	0.03105	1.315
2	$8(3^{\mathrm{f}})$	7/2	4_{31}	B_2	1	5/2	3_{21}	B_1	361.146	10754.638	0.02464	1.052
2	$8(3^{\mathrm{f}})$	11/2	5_{33}	B_2	1	9/2	4_{23}	B_1	422.314	10762.240	0.02850	0.977
2	$8(3^{\mathrm{e}})$	9/2	5_{33}	B_2	1	7/2	4_{23}	B_1	420.631	10765.232	0.02538	0.876
3	$8(1^{\mathrm{e}})$	9/2	4_{13}	B_2	1	11/2	5_{05}	B_1	220.750	11107.460	0.01032	0.754
3	$8(1^{\mathrm{f}})$	19/2	9_{19}	B_2	1	19/2	9_{09}	B_1	659.289	11146.342	0.07678	1.163
3	$8(1^{\mathrm{e}})$	17/2	9_{19}	B_2	1	17/2	9_{09}	B_1	659.280	11146.523	0.06364	0.964
3	$8(1^{\mathrm{f}})$	15/2	7_{17}	B_2	1	15/2	7_{07}	B_1	411.254	11157.266	0.06152	2.275
3	$8(1^{\mathrm{e}})$	13/2	7_{17}	B_2	1	13/2	7_{07}	B_1	411.249	11157.467	0.05229	1.934
3	$8(1^{\mathrm{f}})$	13/2	6_{16}	A_2	1	13/2	6_{06}	A_1	308.767	11161.990	0.05295	0.944
3	$8(1^{\mathrm{e}})$	11/2	6_{16}	A_2	1	11/2	6_{06}	A_1	308.763	11162.200	0.04456	0.795
3	$8(1^{\mathrm{f}})$	11/2	5_{15}	B_2	1	11/2	5_{05}	B_1	220.750	11166.010	0.04378	3.216
3	$8(1^{\mathrm{e}})$	9/2	5_{15}	B_2	1	9/2	5_{05}	B_1	220.747	11166.234	0.03592	2.638
3	$8(1^{\mathrm{f}})$	9/2	4_{14}	A_2	1	9/2	4_{04}	A_1	147.281	11169.170	0.03408	1.087
3	$8(1^{\mathrm{e}})$	7/2	4_{14}	A_2	1	7/2	4_{04}	A_1	147.279	11169.412	0.02691	0.858
3	$8(1^{\mathrm{f}})$	7/2	3_{13}	B_2	1	7/2	3_{03}	B_1	88.424	11171.314	0.02416	2.858
3	$8(1^{\mathrm{e}})$	5/2	3_{13}	B_2	1	5/2	3_{03}	B_1	88.422	11171.563	0.01764	2.087
3	$8(1^{\mathrm{f}})$	3/2	1_{11}	B_2	1	3/2	1_{01}	B_1	14.749	11172.333	0.00739	1.139
3	$8(1^{\mathrm{f}})$	3/2	1_{11}	B_2	1	3/2	1_{01}	B_1	14.749	11187.758	0.00498	0.769
3	$8(1^{\mathrm{e}})$	5/2	2_{11}	B_2	1	3/2	1_{01}	B_1	14.749	11198.827	0.00596	0.921
3	$8(1^{\mathrm{e}})$	5/2	2_{11}	B_2	1	3/2	1_{01}	B_1	14.749	11214.662	0.00773	1.197
3	$8(1^{\mathrm{e}})$	9/2	4_{13}	B_2	1	7/2	3_{03}	B_1	88.424	11239.787	0.01452	1.728
3	$8(1^{\mathrm{f}})$	7/2	4_{13}	B_2	1	5/2	3_{03}	B_1	88.422	11239.928	0.01125	1.339
3	$8(1^{\mathrm{e}})$	13/2	6_{15}	B_2	1	11/2	5_{05}	B_1	220.750	11264.433	0.02081	1.542
3	$8(1^{\mathrm{f}})$	11/2	6_{15}	B_2	1	9/2	5_{05}	B_1	220.747	11264.659	0.01713	1.269
3	$8(1^{\mathrm{f}})$	15/2	8_{17}	B_2	1	13/2	7_{07}	B_1	411.249	11289.313	0.02132	0.798
3	$9(2^{\mathrm{e}})$	11/2	5_{24}	B_1	0	11/2	5_{14}	B_2	289.415	12137.169	0.01344	0.838
3	$9(2^{\mathrm{f}})$	17/2	8_{26}	B_1	0	17/2	8_{18}	B_2	576.821	12140.762	0.03643	0.808
3	$9(2^{\mathrm{f}})$	13/2	6_{24}	B_1	0	13/2	6_{16}	B_2	362.880	12146.585	0.02335	1.119
3	$9(2^{\mathrm{e}})$	11/2	6_{24}	B_1	0	11/2	6_{16}	B_2	362.415	12148.486	0.02009	0.964
3	$9(2^{\mathrm{f}})$	9/2	4_{22}	B_1	0	9/2	4_{14}	B_2	205.731	12150.308	0.01249	1.053
3	$9(2^{\mathrm{e}})$	7/2	4_{22}	B_1	0	7/2	4_{14}	B_2	205.057	12153.123	0.01032	0.873
4	$9(0^{\mathrm{f}})$	9/2	4_{04}	B_1	0	11/2	5_{14}	B_2	289.415	12169.365	0.01689	1.056
4	$9(0^{\mathrm{e}})$	7/2	4_{04}	B_1	0	9/2	5_{14}	B_2	288.851	12169.906	0.01405	0.880
3	$9(2^{\mathrm{f}})$	5/2	2_{20}	B_1	0	3/2	1_{10}	B_2	78.164	12179.758	0.00665	0.890
3	$9(2^{\mathrm{e}})$	7/2	3_{22}	B_1	0	5/2	2_{12}	B_2	105.735	12194.376	0.00867	1.052
3	$9(2^{\mathrm{f}})$	5/2	3_{22}	B_1	0	3/2	2_{12}	B_2	104.472	12198.370	0.00646	0.787
3	$9(2^{\mathrm{f}})$	9/2	4_{22}	B_1	0	7/2	3_{12}	B_2	153.483	12202.555	0.00869	0.888
4	$9(0^{\mathrm{f}})$	5/2	2_{02}	B_1	0	7/2	3_{12}	B_2	153.483	12205.325	0.01198	1.225
4	$9(0^{\mathrm{e}})$	3/2	2_{02}	B_1	0	5/2	3_{12}	B_2	152.599	12206.190	0.00858	0.881
3	$9(2^{\mathrm{e}})$	11/2	5_{24}	B_1	0	9/2	4_{14}	B_2	205.731	12220.852	0.01115	0.946
3	$9(2^{\mathrm{f}})$	9/2	5_{24}	B_1	0	7/2	4_{14}	B_2	205.057	12223.267	0.00916	0.779
4	$9(0^{\mathrm{f}})$	1/2	0_{00}	B_1	0	3/2	1_{10}	B_2	78.164	12237.912	0.00707	0.951
4	$9(0^{\mathrm{f}})$	9/2	4_{04}	B_1	0	9/2	4_{14}	B_2	205.731	12253.049	0.02348	1.997
4	$9(0^{\mathrm{f}})$	5/2	2_{02}	B_1	0	5/2	2_{12}	B_2	105.735	12253.073	0.01479	1.803
4	$9(0^{\mathrm{e}})$	7/2	4_{04}	B_1	0	7/2	4_{14}	B_2	205.057	12253.699	0.01889	1.611
4	$9(0^{\mathrm{f}})$	13/2	6_{06}	B_1	0	13/2	6_{16}	B_2	362.880	12253.774	0.02945	1.424
4	$9(0^{\mathrm{e}})$	11/2	6_{06}	B_1	0	11/2	6_{16}	B_2	362.415	12254.207	0.02521	1.221
4	$9(0^{\mathrm{e}})$	3/2	2_{02}	B_1	0	3/2	2_{12}	B_2	104.472	12254.317	0.00954	1.168
4	$9(0^{\mathrm{f}})$	9/2	4_{04}	B_1	0	7/2	3_{12}	B_2	153.483	12305.297	0.00962	0.992
4	$9(0^{\mathrm{e}})$	7/2	4_{04}	B_1	0	5/2	3_{12}	B_2	152.599	12306.157	0.00741	0.767
4	$9(0^{\mathrm{f}})$	13/2	6_{06}	B_1	0	11/2	5_{14}	B_2	289.415	12327.239	0.01623	1.028
4	$9(0^{\mathrm{e}})$	11/2	6_{06}	B_1	0	9/2	5_{14}	B_2	288.851	12327.771	0.01364	0.866

Although CH_2^+ is a simple molecule, and the level of *ab initio* theory we have used is high, the potentials obtained are not good enough to enable us to calculate accurately $\tilde{X}$ state levels at energies around 11 000 cm^{-1} so that we can quantitatively account for the perturbation that the $\tilde{A}$ 8(1) vibronic state suffers. Further, because perturbations are very sensitive to small changes in potential function parameters, in order to achieve a satisfactory fitting to the observed position of the perturbed lines, the initial potentials have to be rather close to optimum, and there should be enough unperturbed data to provide a significant level of constraint for the fitting process. In this latter regard, it would be a great help to have experimental information giving the positions of more vibrational energy levels of $\tilde{X}$-state CH_2^+, and to have more bands assigned and analysed in the $\tilde{A} \leftarrow \tilde{X}$ electronic band system. With improved initial potentials, and more experimental input data, we would be able to vary more parameters in the least-squares fitting. This would not only improve the agreement with experiment for the perturbed $\tilde{A}$ 8(1) energy levels, but also lower the residuals for the unperturbed energy separations. For these separations, we obtain here typical residuals of a few cm^{-1}. However, the accuracy that could ideally be obtained with our model is probably somewhat better than that, as suggested by the fact that for the electronic ground state of water (which, admittedly, does not exhibit the Renner effect), a fitting to 550 energy level separations, involving rotation–vibration states with $J \leq 2$ in 103 vibrational states of six isotopologues, produced a standard deviation of 0.63 cm^{-1} [32]; this fitting used a model analogous to that of the present work.

This work was supported by the European Commission through contract no. MRTN-CT-2004-512202 'Quantitative Spectroscopy for Atmospheric and Astrophysical Research' (QUASAAR). The work of PJ is supported in part by the Deutsche Forschungsgemeinschaft and the Fonds der Chemischen Industrie.

References

[1] W. P. Kraemer, P. Jensen, and P. R. Bunker, Can. J. Phys. **72**, 871 (1994).
[2] P. Jensen, M. Brumm, W. P. Kraemer, and P. R. Bunker, J. Molec. Spectrosc. **172**, 194 (1995).
[3] G. Osmann, P. R. Bunker, P. Jensen and W. P. Kraemer, Chem. Phys. **225**, 33 (1997).
[4] G. Osmann, P. R. Bunker, W. P. Kraemer, and P. Jensen, Chem. Phys. Lett. **309**, 299 (1999).
[5] G. Osmann, P. R. Bunker, W. P. Kraemer, and P. Jensen, Chem. Phys. Lett. **318**, 597 (2000).
[6] P. R. Bunker, M. C. Chan, W. P. Kraemer, and P. Jensen, Chem. Phys. Lett. **341**, 358 (2001).
[7] P. Jensen, T. E. Odaka, W. P. Kraemer, T. Hirano, and P. R. Bunker, Spectrochim. Acta Part A **58**, 763 (2002).
[8] P. Jensen, S. S. Wesolowski, N. R. Brinkmann, N. A. Richardson, Y. Yamaguchi, H. F. Schaefer III, and P. R. Bunker, J. Molec. Spectrosc. **211**, 254 (2002).
[9] P. R. Bunker, W. P. Kraemer, P. Jensen, Y.-C. Lee, and Y.-P. Lee, J. Molec. Spectrosc. **216**, 419 (2002).
[10] S. N. Yurchenko, P. R. Bunker, and P. Jensen, J. Molec. Struc. **742**, 43 (2005).
[11] P. Jensen, M. Brumm, W. P. Kraemer, and P. R. Bunker, J. Molec. Spectrosc. **171**, 31 (1995).
[12] M. Kolbuszewski, P. R. Bunker, W. P. Kraemer, G. Osmann, and P. Jensen, Molec. Phys. **88**, 105 (1996).
[13] P. R. Bunker and P. Jensen, *Molecular Symmetry and Spectroscopy*, 2nd ed. (NRC Research Press, Ottawa, Canada, 2006).
[14] M. Rösslein, C. M. Gabrys, M.-F. Jagod, and T. Oka, J. Molec. Spectrosc. **153**, 738 (1992).
[15] J. L. Gottfried and T. Oka, J. Chem. Phys. **121**, 11527 (2004).
[16] C. M. Gabrys, D. Uy, M.-F. Jagod, and T. Oka, private communication (1994). See table IV of [2].
[17] C. F. Neese, J. L. Gottfried, C. P. Morong, and T. Oka, in preparation.
[18] S. Willitsch, L. L. Imbach, and F. Merkt, J. Chem. Phys. **117**, 1939 (2002).
[19] S. Willitsch and F. Merkt, J. Chem. Phys. **118**, 2235 (2003).
[20] G. D. Purvis and R. J. Bartlett, J. Chem. Phys. **76**, 1910 (1982).
[21] M. Urban, J. Noga, S. J. Cole, and R. J. Bartlett, J. Chem. Phys. **83**, 4041 (1985).
[22] K. Raghavachari, G. W. Trucks, J. A. Pople, and M. Head-Gordon, Chem. Phys. Lett. **157**, 479 (1989).
[23] H.-J. Werner and P. J. Knowles, MOLPRO version 2002.6, a package of *ab initio* programs. It is based on previous versions by R. D. Amos, A. Bernhardsson, A. Berning, P. Celani, D. L. Cooper, M. J. O. Deegan, A. J. Dobbyn, F. Eckert, C. Hampel, G. Hetzer, P. J. Knowles, T. Korona, R. Lindh, A. W. Lloyd, S. J. McNicholas, F. R. Manby, W. Meyer, M. E. Mura, A. Nicklass, P. Palmieri, R. Pitzer, G. Rauhut, M. Schütz, U. Schumann, H. Stoll, A. J. Stone, R. Tarroni, T. Thorsteinsson, and H.-J. Werner.
[24] C. Hampel, K. Peterson, and H.-J. Werner, Chem. Phys. Lett. **190**, 1 (1992)
[25] M. J. O. Deegan and P. J. Knowles, Chem. Phys. Lett. **227**, 321 (1994).
[26] T. H. Dunning, J. Chem. Phys. **90**, 1007 (1989).
[27] R. A. Kendall, T. H. Dunning, and R. J. Harrison, J. Chem. Phys. **96**, 6796 (1992).
[28] D. Feller, J. Chem. Phys. **96**, 6104 (1992).
[29] H.-J. Werner and P. J. Knowles, J. Chem. Phys. **89**, 5803 (1988).
[30] P. J. Knowles and H.-J. Werner, Chem. Phys. Lett. **145**, 514 (1988).
[31] T. H. Dunning, J. Chem. Phys. **55**, 716 (1971).
[32] P. Jensen, J. Molec. Spectrosc. **133**, 438 (1989).